Phylogeography of bar-tailed godwits: pre-LGM structure in Beringia and westward colonization of post-glacial Europe

Jesse R. Conklin[1,2*], Yvonne I. Verkuil[1,2], Margaux J.M. Lefebvre[3], Phil F. Battley[4], Roeland A. Bom[2,5], Robert E. Gill, Jr.[6], Chris J. Hassell[7], Job ten Horn[5], Daniel R. Ruthrauff[6], T. Lee Tibbitts[6], Pavel S. Tomkovich[8], Nils Warnock[9], Theunis Piersma[1,2,5] & Michaël C. Fontaine[1,3]

[1]Groningen Institute for Evolutionary Life Sciences (GELIFES), University of Groningen, P.O. Box 11103, 9700 CC Groningen, The Netherlands

[2]BirdEyes, Centre for Global Ecological Change at the Faculties of Science & Engineering and Campus Fryslân, University of Groningen, Zaailand 110, 8911 BN Leeuwarden, The Netherlands

[3]MiVEGEC, CNRS, IRD, University of Montpellier, Montpellier, France

[4]Zoology and Ecology Group, Massey University, Palmerston North 4442, New Zealand

[5]Department of Coastal Systems, NIOZ Royal Netherlands Institute for Sea Research, P.O. Box 59, 1790 AB Den Burg, Texel, The Netherlands

[6]U.S. Geological Survey, Alaska Science Center, 4210 University Drive, Anchorage, AK 99508, USA

[7]Global Flyway Network, PO Box 3089, Broome, WA 6725, Australia

[8]Zoological Museum, Moscow MV Lomonosov State University, Bolshaya Nikitskaya Str. 6, Moscow 125009, Russia

[9]Audubon Canyon Ranch, Cypress Grove Research Center, Marshall, CA 94940, USA

*Corresponding author: conklin.jesse@gmail.com

ABSTRACT

In migratory birds, high mobility may reduce population structure through increased dispersal and enable adaptive responses to environmental change, whereas rigid migratory routines predict low dispersal, increased geographic structure, and limited flexibility to respond to change. We used nextRAD sequencing of 14,318 single-nucleotide polymorphisms to explore the population genetics and phylogeographic history of the bar-tailed godwit, *Limosa lapponica*, a migratory shorebird with six recognized subspecies and known for making the longest non-stop flights of any landbird. Using scenario-testing in an Approximate Bayesian Computation framework, we infer that bar-tailed godwits existed in three main lineages at the Last Glacial Maximum (LGM), when much of their present-day Arctic and sub-Arctic breeding range persisted in a large, unglaciated Siberian-Beringian refugium. Subsequently, population structure developed at both longitudinal extremes: in the east, a genetic cline exists across latitude in the Alaska breeding range of subspecies *L. l. baueri*; in the west, one lineage diversified into three extant subspecies *L. l. lapponica*, *taymyrensis*, and *yamalensis*, the former two of which migrate through previously glaciated western Europe. We also detected unrecognized population structure among bar-tailed godwits wintering in Europe, wherein a significant proportion of purported *lapponica* individuals were in fact *taymyrensis*, necessitating a re-assessment of the migrations, ecology, and population estimates for these subspecies. In the global range of this long-distance migrant, we found evidence of both (1) fidelity to rigid behavioral routines promoting fine-scale geographic population structure (in the east), and (2) flexibility to colonize recently available migratory flyways and non-breeding areas (in the west).

1 | INTRODUCTION

Animal migration is shaped by, and dependent upon, resources and conditions that vary spatially and seasonally (Alerstam et al., 2003), and therefore migratory populations are considered particularly vulnerable to disruptions caused by climate change and anthropogenic habitat modification (Kubelka et al., 2022; Robinson et al., 2009). In birds, migration involves a highly integrated, multi-trait phenotype (including flight capacity, fueling, navigation, molt, etc.; Piersma et al., 2005) and some degree of endogenous behavioral control (Åkesson et al., 2017; Åkesson & Helm, 2020) that may imply limited flexibility to adapt to conditions outside those in which the migration evolved. Conversely, it is clear that some migratory bird populations have persisted through historical large-scale environmental perturbations, such as repeated Pleistocene glaciations (Batchelor et al., 2019; Hewitt, 2000); apparent responses included population sub-division and size changes, loss and gain of migration, and altered migration routes and distances (e.g., Avise & Walker, 1998; Conklin et al., 2022; Milá et al., 2006; Tan et al., 2023; Zink & Gardner, 2017). A phylogeographic approach (Avise, 2009; Knowles & Maddison, 2002) can help us understand what perturbations migratory populations have survived in the past, and therefore their potential resiliance to future changes.

The bar-tailed godwit, *Limosa lapponica*, is a migratory shorebird (Order Charadriiformes, Family Scolopacidae) that breeds on Arctic and sub-Arctic tundra from Scandinavia east to Alaska, and spends the non-breeding season on intertidal mudflats from West Africa to New Zealand (Figure 1). There are up to six recognized subspecies of bar-tailed godwits, with distinct breeding areas and migratory routes (Figure 1), and further distinguished by variation in plumage and body size (Bom et al., 2022; Engelmoer & Roselaar, 1998; Tomkovich,

2010). Based on non-breeding census data, population sizes for these subspecies vary from c. 100,000 to 500,000 individuals (Wetlands International, 2023), except for the subspecies *L. l. anadyrensis*, which has a poorly described non-breeding range (Chan et al., 2022) but is believed to number <10,000 individuals. The species is considered Near Threatened by the IUCN based on widespread population declines, particularly associated with limitations at migratory stopover sites (Rakhimberdiev et al., 2018; Studds et al., 2017), although the nominate European-wintering population *L. l. lapponica* is thought to be increasing (BirdLife International, 2023).

In the western Palearctic, the present-day ranges of three bar-tailed godwit subspecies (*lapponica*, *taymyrensis*, and *yamalensis*) were strongly affected by the glaciation of Europe during the last glacial maximum (LGM, c. 20,000–25,000 years before present, ybp; Hewitt, 2000). Accordingly, these three subspecies were indistinguishable at the mtDNA Control Region (Bom et al., 2022), suggesting a recent postglacial radiation into three migration routes (Figure 1). In particular, the entire present-day breeding range of *lapponica*, which makes the shortest migration in the species (one-way distance of c. 2,500–4,500 km), was unavailable at the LGM, making it presumably the youngest subspecies.

By contrast, the eastern part of the bar-tailed godwit breeding range falls within Beringia, an area of the Arctic that stretches from the Lena River in northeast Russia to the Mackenzie River in northwest Canada (Figure 1) and was largely ice-free at the LGM (Ehlers & Gibbard, 2007; Pielou, 1991) and previous glacial cycles (Batchelor et al., 2019). The much deeper biogeographical history of this region, which includes the periodic appearance and disappearance of the Bering Land Bridge, connecting North America with Asia, is reflected in complex histories of diversification in many Beringian taxa (Winker et al., 2023). Thus,

two eastern subspecies (*menzbieri* and *baueri*) could have persisted near their present-day ranges for much longer than the western subspecies, and indeed show deeper divergences at the mitochondrial control region (mtDNA) (Bom et al., 2022). A latitudinal cline in both morphology and annual-schedule timing across Alaska (Conklin et al., 2010, 2011) suggests that additional population genetic structure may exist within *baueri*. Conversely, the small breeding range of *anadyrensis* in Chukotka (Figure 1) was at least partly glaciated at the LGM (Batchelor et al., 2019), and therefore could represent a recent expansion into newly available breeding habitat.

Of particular interest is the evolution and persistence of the migration of the *baueri* subspecies, which includes three separate trans-oceanic flights of >5,000 km, including a southward flight of c. 12,000 km across the Pacific Ocean from Alaska to New Zealand (Figure 1), the longest non-stop flight recorded in any landbird (Conklin et al., 2017; Gill et al., 2009). Given this annual routine's apparent reliance on the specific distribution of habitats and environmental conditions around the Pacific (Conklin et al., 2017; Gill et al., 2014; Piersma et al., 2022), it is unclear how long godwits have been making this migration, and whether it will withstand major changes (e.g. in habitat, prevailing winds etc.) in the future. Unraveling the history of bar-tailed godwits may help reveal whether the trans-Pacific migratory route, and the physiological capabilities required to use it, arose *in situ*, or were products of eastward expansion from the Palearctic (Hedenström, 2010; Piersma et al., 2022).

In this study, we describe the history of divergences and degree of neutral genetic differentiation among global flyway populations of bar-tailed godwits. We used nextera-tagmented, reductively-amplified DNA (nextRAD) sequencing (Russello et al., 2015) for *de novo* discovery of genome-wide single-nucleotide polymorphisms (SNPs) for population

genetic analyses, and compared hypothesized evolutionary scenarios in an Approximate Bayesian Computation (ABC) framework using DIYABC-RF (Collin et al., 2021). By reconstructing the recent evolutionary history of bar-tailed godwits, we (1) identify previously unrecognized sub-specific structure, (2) reveal the divergence times and historical connections among populations, and (3) provide insights regarding the origins and maintenance of population structure in long-distance migratory birds.

2 | MATERIALS AND METHODS

2.1 | Sampling and DNA extraction

We assembled DNA samples representing all recognized and hypothesized breeding populations within the global range of bar-tailed godwits (Figure 1, Table S1). Where possible, we used samples collected in known breeding areas; however, because bar-tailed godwits breed in low densities in remote regions, for some populations there were few or no breeding samples available. In these cases, we used samples collected from non-breeding sites when sampled individuals could be confidently assigned to breeding areas either because they were remotely tracked to breeding areas using satellite-telemetry or light-level geolocation, or because long-term research programs had established strong links between breeding and non-breeding areas (e.g. through mark-recapture/resight programs). There were no verifiable samples available from the poorly-studied *anadyrensis* population; however, godwits have been collected from coastal southeast Chukotka, within 300 km of the known *anadyrensis* breeding range (Tomkovich, 2010) and far from the expected migration routes of *menzbieri* and *baueri* (Figure 1). Therefore, we included eight such samples, in order to detect genetic variation that might indicate the distinctiveness of *anadyrensis*. All tissue

148 samples were acquired from museum collections or collected by the authors and colleagues in
149 the field under all requisite permits appropriate to their respective countries and institutions.
150
151 We extracted genomic DNA from samples using two methods. For blood or organ tissue
152 samples preserved in 95% ethanol, we used the DNeasy Blood and Tissue Kit (Qiagen)
153 following the manufacturer's instructions for tissue. For blood samples preserved in Queen's
154 lysis buffer, we used the NucleoSpin Blood QuickPure Kit (Macherey-Nagel). Extract quality
155 was first assessed on a 1.5% agarose gel to exclude extractions with insufficient yield or
156 excessively degraded DNA. We then quantified DNA concentrations using a Qubit 3.0
157 fluorometer (Life Technologies), diluted extracts to achieve relatively even concentrations,
158 and dried down samples in a SpeedVac concentrator (ThermoFisher Scientific). We delivered
159 80–162 ng of DNA of 209 individual godwits (Table S1) for SNP discovery and genotyping.
160
161 **2.2 | SNP genotyping using nextRAD sequencing**
162 Genomic DNA was converted into nextRAD genomic fragment libraries (SNPsaurus, LLC,
163 USA) following the method described by Russello et al. (2015). Genomic DNA was first
164 fragmented with Nextera reagent (Illumina, Inc.), which also ligates short adapter sequences
165 to the ends of the fragments. The Nextera reaction was scaled for fragmenting 10 ng
166 of genomic DNA, although 20–30 ng of genomic DNA was used for input to compensate for
167 degraded DNA in the samples and to increase fragment sizes. Fragmented DNA was then
168 amplified, with one of the primers matching the adapter and extending 10 nucleotides into
169 the genomic DNA with the selective sequence 'GTGTAGAGCC'. Thus, only fragments
170 starting with a sequence that can be hybridized by the selective sequence of the primer were
171 efficiently amplified. PCR amplification was done at 74°C for 27 cycles. The nextRAD

172 libraries were sequenced on an Illumina HiSeq-4000 at the Genomics Core Facility,
173 University of Oregon, USA.
174
175 For SNP-calling, reads were first trimmed using custom scripts (SNPsaurus, LLC) in bbduk
176 (BBMap tools; Bushnell, 2016). Next, a *de novo* reference was created from abundant reads
177 (after removal of low-quality (phred-scale quality <20) and very high-abundance reads) and
178 reads that aligned to these. All 205,854,244 reads were mapped to the reference with an
179 alignment identity threshold of 95% using bbmap (BBMap tools). Genotype calling was
180 performed using SAMtools and BCFtools (samtools mpileup -gu -Q 10 -t DP, DPR -f
181 ref.fasta -b samples.txt | bcftools call -cv - > genotypes.vcf), applying a minimum read depth
182 filter of 7x. The genotype table was then filtered using VCFtools v.01.14 (Danecek et al.,
183 2011) to remove SNPs called in <80% of samples and putative alleles with a population
184 frequency <3%, to exclude artefactual variants. The resulting VCF file included 6,424 unique
185 loci (150-bp sequences) containing 21,031 SNPs.
186
187 Additional cleaning was performed using VCFtools to remove indels (n = 478 SNPs), low-
188 quality SNPs (phred-scale quality [QUAL] <999; n = 15 SNPs), and samples that failed to
189 sequence (n = 1 *menzbieri* individual) or were of unknown breeding population (n = 9
190 individuals from New Zealand that could not be confidently assigned to a breeding region
191 within Alaska based on tracking data). Next, SNPs deviating from Hardy-Weinberg (H-W)
192 proportions in all seven hypothesized populations (excluding *anadyrensis*) were identified
193 and removed using VCFtools ($p < 0.05$; n = 48 SNPs); the small sample size in *anadyrensis*
194 made it statistically insensitive to H-W deviations. To ensure independence of loci, we used
195 PLINK v.1.9 (Chang et al., 2015) to identify and remove all SNPs in linkage disequilibrium

196 (LD; r^2 >0.20; n = 6,188 SNPs). The LD-pruned data set included 199 individuals and 14,318
197 unlinked SNPs on 6,140 loci.
198
199 We then used VCFtools to calculate proportion of missing SNP calls per individual (range 1–
200 77%) and removed 15 individuals with >30% missing data. Because inclusion of related
201 individuals can bias population genetic analyses (Anderson & Dunham, 2008; Rodríguez-
202 Ramilo & Wang, 2012), we estimated individual pairwise relatedness in PLINK using the
203 Identity-by-Descent estimator PI HAT; we found no cases of relatedness involving half-
204 siblings or closer (PI HAT >0.20). The final data set included 184 individuals and 14,318
205 SNPs. We used VCFtools, PLINK, and PGDspider v.2.1.0.3 (Lischer & Excoffier, 2012) to
206 convert data to different formats required for further analysis.
207
208 **2.3 | Inference of population structure and diversity**
209 To assess major axes of genetic variation and structure, we performed a principal component
210 analysis (PCA; Patterson et al. 2006) using the R packages *gdsfmt* v.1.14.1 and *SNPRelate*
211 v.1.12.2 (Zheng et al., 2012). We determined the number of ancestral populations or clusters
212 (K) and ancestry proportions of these for each individual using ADMIXTURE v.1.3.0
213 (Alexander et al., 2009). We conducted 20 replicate runs (with random seeds) for each
214 putative number of clusters (K) ranging from 1 to 8. We used cross-validation (CV)
215 (Alexander & Lange, 2011) to assess how the CV error rate varied with increasing K values
216 and which value provided the lowest CV error. Then, we used the CLUMPAK (Cluster
217 Markov Packager Across K; Kopelman et al., 2015) web server (http://clumpak.tau.ac.il/)
218 with default settings to summarize estimates of individual ancestry proportions to each
219 cluster across replicate runs, inspect potential distinct solutions identified, and visualize the
220 most likely ancestry proportions at each value of K.

Globally and for each putative population, we characterized genetic diversity by calculating nucleotide diversity (π), heterozygosity, and inbreeding coefficient (F_{IS}) using VCFtools. We evaluated evidence for deviations from mutation-drift equilibrium, indicative of departures from a null hypothesis of constant population size, by estimating the per-locus Tajima's *D* values for each population using VCFtools. We estimated the degree of genetic differentiation among populations by calculating pairwise F_{ST} (Weir & Cockerham, 1984) using the *diffCalc* function in the R package *diversity* v.1.9.90 (Keenan et al., 2013), with 95% confidence intervals derived from 500 bootstraps. We calculated *p*-values for F_{ST} estimates using the *pairwiseTest* function (1,000 permutations) in the R package *strataG* v.2.4.905 (Archer et al., 2017).

2.4 | Population evolutionary relationships and demographic history

To visualize evolutionary relationships among populations, we first constructed a midpoint-rooted neighbor-joining tree based on Nei's genetic distance (Nei, 1972) using the R packages *poppr* v.2.8.5 (Kamvar et al., 2014) and *ape* v.5.3 (Paradis & Schliep, 2019), with missing data replaced by mean allele counts, and node support calculated from 1,000 bootstraps.

To identify likely potential sources of admixture in the tree, we first conducted the three-population test for admixture (Reich et al., 2009) in R using ADMIXTOOLS 2.0.0 (Maier et al., 2023) for all possible population triads. Briefly, the f_3 statistic (Patterson et al., 2012) assesses shared genetic drift to test the null hypothesis that a target population (A) is related to two other populations (B, C) in a simple tree-like manner. We tested significance of the f_3 test using a blocked-jackknife resampling of SNPs, considering blocks of 100 SNPs. A

246 significantly negative value of f_3 (A;(B,C)) indicates that the target population must have
247 arisen from an admixture of the other two populations, or populations closely related to them.
248
249 To further investigate the genetic relationships among godwit populations, we estimated
250 population networks using the approach implemented in ADMIXTOOLS 2.0.0 (Maier et al.,
251 2023), which uses the shared and private genetic ancestry components of genome-wide allele
252 frequency data to infer population branching while accounting for potential historical
253 migration and admixture events among populations. To find the best network topology, we
254 used the function *find_graphs* for 0 to 5 admixture events (*m*), each with 100 replicates and a
255 maximum of 300 generations. For each replicate, we calculated the out-of-sample score to
256 account for the difference in likelihood score caused by an increasing number of admixture
257 events, which also increase the degrees of freedom. We used the *baueri* South population as a
258 root to fold the networks; even if that population is not an actual outgroup, it allowed
259 visualizing population relationships in a consistent way. The actual population branching
260 order was later assessed statistically using the Approximate Bayesian Computation (ABC)
261 (Beaumont et al., 2002) Random Forest (RF) statistical framework (Pudlo et al., 2016;
262 Raynal et al., 2019). For the best-supported replicates (i.e., those displaying the likelihood
263 score closest to zero), we assessed the goodness-of-fit with the R package *admixture-graph*
264 v.1.0.2 (Leppälä et al., 2017). This approach allows comparing the observed and expected
265 values of f_4 statistics among the different alternatives and identifying the graph that best fits
266 the data (i.e., the one properly predicting the observed f_4 values for all possible four-
267 population combinations).
268
269 Finally, we evaluated the support for different possible scenarios of population divergence
270 and admixture using the ABC-RF statistical framework (Pudlo et al., 2016; Raynal et al.,

271 2019) in the R package DIYABC-RF v.1.2.1 (Collin et al., 2021). ABC-RF can estimate
272 posterior probabilities of historical scenarios, based on massive coalescent simulations of
273 genetic data. Simulations are compared to observed SNP data using summary statistics to
274 identify the best-fitting model by calculating the number of RF votes and to approximate the
275 posterior probability for the best model (Pudlo et al., 2016). The best-fitting posterior
276 parameter distribution values for the best model can be estimated using a RF procedure
277 applied in a regression setting (Raynal et al., 2019). Estimated parameters include the
278 effective size (N_e) for each population, admixture events and their rates (r), and split and
279 admixture times (t). We evaluated potential evolutionary scenarios in a stepwise manner, as
280 follows.
281
282 As our primary question arising from the above analyses concerned the nature and relative
283 timing of the admixed origin of *menzbieri* (see *Results*), we sought to first reduce the number
284 of potential scenarios by fixing the topology of the relationships among the three *baueri*
285 populations. So, in Step 1, we tested whether the apparently clinal variation among these
286 populations was best represented by one of two possible simple branching topologies or with
287 *baueri* Central as an admixture of *baueri* North and South (Figure S4, Table S2).
288
289 In Step 2, we created four possible scenarios (Figure S5c–f) for an admixed origin of
290 *menzbieri* from neighboring populations to the west and east, while allowing populations on
291 the two main branches to diverge at different times relative to each other. Essentially, the
292 admixed origin of *menzbieri* could occur: 1) before either branch began to diverge (Figure
293 S5c); 2) after populations on one branch diverged but before the other branch began to
294 diverge (Figure S5d,e); or 3) after populations on both branches had diverged (Figure S5f).
295 To compete with these scenarios, we created two "null-hypothesis" scenarios in which

296 *menzbieri* was not admixed, but simply diverged from one of the two main branches (Figure
297 S5a,b).
298
299 The scenario parameters were considered as random variables drawn from prior distributions
300 (Tables S2 and S3). We used DIYABC-RF to simulate 20,000 genetic data sets per scenario,
301 with the same properties as the observed data set (number of loci and proportion of missing
302 data). Simulated and observed data sets were summarized using the whole set of summary
303 statistics proposed by DIYABC-RF for SNP markers (Table S4), describing population
304 genetic variation (e.g. heterozygosity, proportion of monomorphic loci), differentiation (e.g.
305 F_{ST} and Nei's genetic distances), or admixture (e.g. admixture coefficient, f_3 and f_4 statistics;
306 Patterson et al., 2012); see the full list and details in Table S4. Linear discriminant analysis
307 (LDA) components were also used as additional summary statistics (Estoup et al., 2012). The
308 total number of summary statistics was 50 and 1,708 for Step 1 and 2, respectively.
309
310 We used the random forest (RF) classification procedure (Pudlo et al., 2016) to compare the
311 likelihood of the competing scenarios at each step with DIYABC-RF. RF is a machine-
312 learning algorithm that uses hundreds of bootstrapped decision trees to perform classification,
313 using the summary statistics as a set of predictor variables. Some simulations are not used in
314 decision tree building at each bootstrap (i.e., the out-of-bag simulations), and are used to
315 compute the "prior error rate," which provides a direct method for estimating the cross-
316 validation error rate. At each step, we built a training set of 20,000 simulated data sets per
317 scenario, with the same number of loci and individuals as the observed data set, and then
318 grew classification forests of increasing size (100, 500, and 2,000 trees) to test convergence.
319 The RF computation provides a classification vote for each scenario (i.e., the number of times
320 a model is selected from the decision trees). We selected the scenario with the highest

classification vote as the most likely scenario, and we estimated its posterior probability following the recommendation of Pudlo et al. (2016). We assessed the global performance of our chosen ABC-RF scenario, by calculating the prior error rate based on the available out-of-bag simulations and we repeated the RF analysis (3 times in Step 1; 10 times in Step 2) to ensure that the results converged.

For the best-supported model in Step 2, we estimated posterior distribution values of all parameters using a regression by RF methodology (Raynal et al., 2019) in DIYABC-RF. We used a classification forest of 500 decision trees, based on a training set of 100,000 simulations, to conduct the parameter estimations. We converted divergence time estimates to years assuming a generation time of 8 years (delayed maturity with adult annual survival c. 0.86; Méndez et al., 2018) and the genome-wide mutation rate calculated by Zhang et al. (2014) for Order Charadriiformes: 1.5×10^{-9} substitutions per site per year. All of the steps involved in the ABC-RF analysis (simulations, computation of summary statistics, model checking, scenario comparisons, and estimations of parameter posterior distributions) were performed with DIYABC-RF.

3 | RESULTS

3.1 | Summary of nextRAD SNP data set

The final data set comprised 184 unrelated bar-tailed godwits genotyped at 14,318 unlinked high-quality SNPs; this included 15–31 individuals in each of seven hypothesized populations, but only three purported *anadyrensis* individuals (Table S1). On average, individuals were genotyped at 93.7% (range: 72–99%) of SNPs and with a mean read depth of 50.4 (range: 15–116). Each SNP was genotyped in an average of 172.5 (range: 149–184,

346 or 81–100%) individuals. Globally, nucleotide diversity (π) was 0.245, and heterozygosity
347 was 20.6%.
348
349 **3.2 | Population structure and diversity**
350 The first three axes (PC1–3) of the principal component analysis explained 4.0% of the total
351 genetic variation (Figure 2a). On PC1, individuals were essentially distributed on an axis of
352 longitude in three clusters: a western Palearctic group containing all of *lapponica,*
353 *taymyrensis* and *yamalensis*; an Alaska group containing all of *baueri*; and an intermediate
354 group of *menzbieri*, suggesting an admixed origin (Figure 2a). PC2 separated 12 *lapponica*
355 individuals from the main western Palearctic cluster. PC3 stretched *baueri* individuals along
356 a latitudinal cline, partly separating the North, South and Central populations. The three
357 purported *anadyrensis* individuals did not form a coherent cluster, one clustering with
358 *menzbieri* and two with *baueri*. Higher-order axes of variation (PC4–6) explained an
359 additional 2.2% of variation but revealed negligible further sub-structure (Figure S1).
360
361 Genetic ancestry analyses with ADMIXTURE for $K = 2$ ancestral populations provided the
362 lowest CV error criterion (Figure S2) and 100% support for the major clusters across 20
363 replicate runs. At $K = 2$, populations were clearly divided between a western Palearctic
364 cluster and an Alaska cluster, with *menzbieri* reflecting admixture between the two (Figure
365 2b). Additional structure identified in the PCA was apparent at $K = 3$ and 4; i.e. the clear
366 structure within purported *lapponica* and the clinal variation within *baueri*, respectively. At K
367 $= 5$, the identification of a predominantly *menzbieri* cluster may suggest significant genetic
368 drift specific to that population, as opposed to an origin of simple and recent admixture.
369 Higher values of K revealed no further important geographic structure (Figure S2). Again, the

370 purported *anadyrensis* individuals did not form a coherent cluster, but appears to include one
371 *menzbieri* and two *baueri* individuals (Figure 2b).
372
373 In both PCA and ADMIXTURE, only 6 of 27 purported *lapponica* individuals sampled on
374 wintering grounds in The Netherlands clearly grouped with the four individuals sampled at
375 known *lapponica* breeding areas in western Russia (see Figure 1, Table S1). Of the remaining
376 21, 19 clearly grouped with *taymyrensis* (sampled at breeding areas in central Russia and a
377 non-breeding area in Mauritania), and two appear to reflect admixture between *lapponica* and
378 *taymyrensis* (Figure 2a,b). Therefore, for further analysis, we considered a new population of
379 '*taymyrensis* Europe' (n = 19), and a reduced *lapponica* population (n = 10 'true' *lapponica*
380 plus the 2 admixed individuals). For clarity, we hereafter refer to the original *taymyrensis*
381 samples as '*taymyrensis* Africa' (n = 29). As PCA and ADMIXTURE results do not support
382 an identifiable *anadyrensis* population, we excluded those samples (n = 3) from further
383 analysis. Therefore, we proceeded with 181 individuals in eight populations.
384
385 Globally, nucleotide diversity was 0.245, and this was similar for all populations (Table S5).
386 Mean heterozygosity was also generally uniform (range of means: 0.198–0.215), with no
387 evidence of inbreeding in any population (all mean F_{IS} < 0.20; Table S5). Values of Tajima's
388 D were low and similar among populations (range of means: 0.214–0.339; Table S5),
389 suggesting no evidence of dramatic population-size changes or additional hidden structure.
390
391 Pairwise F_{ST} among the eight hypothesized populations ranged 0.001–0.048 (Table 1), and
392 were greatest between the westernmost and easternmost breeding populations (*lapponica* vs.
393 *baueri;* F_{ST} values ranging from 0.046 to 0.048 for the three *baueri* sub-populations). The
394 two groups that winter in Europe, all previously considered *lapponica* (*lapponica* and

395 *taymyrensis* Europe), were moderately differentiated (F_{ST} = 0.016). Differentiation among the
396 three sub-populations of *baueri* (F_{ST} = 0.006–0.009) was lower than for most recognized
397 subspecies pairs, with 95% CIs that included zero. The lowest values were among the three
398 groups breeding in central Russia (*taymyrensis* Europe, *taymyrensis* Africa, and *yamalensis*;
399 F_{ST} = 0.001–0.003).
400
401 **3.3 | Population evolutionary relationships and demographic history**
402 The neighbor-joining (NJ) tree based on Nei's distance (Figure 3a) again identified two main
403 branches (western Palearctic and Alaska groups), with low node support within each group,
404 and *menzbieri* occupying an intermediate position between them.
405
406 The three-population test (based on the Patterson's f_3 statistic of the form (A;(B,C)); Table
407 S6) identified *menzbieri* as a likely product of admixture between the two main branches
408 identified by the NJ tree (see Figure 3a). Of 168 possible population triads, 12 produced a
409 significantly negative f_3 statistic; all of these included *menzbieri* as the target population (A)
410 and one member of each of the two main branches (*lapponica/taymyrensis/yamalensis* or the
411 *baueri* group, respectively) as the source populations (B, C) (Table S6).
412
413 For admixture graphs estimated by ADMIXTOOLS 2, the greatest increase in likelihood
414 occurred at m = 2 admixture edges in the population graph (Figure S3a), but out-of-sample
415 scores indicated the highest likelihood at m = 3 (Figure S3b). Overall, the five best-supported
416 replicates (i.e., those with likelihood scores closest to zero) included two distinct network
417 topologies for m = 3 and one for m = 2. The best-supported topologies at m = 2 and 3 (Figure
418 S3c,d) each provided a perfect fit with the data as estimated by *Admixture-graph* (i.e., no
419 outlying observed f_4 statistic values compared to those theoretically expected from these

420 graphs; Figure S3e,f). Therefore, according to parsimony we present the model at $m = 2$
421 (Figure 3b). In this graph, *menzbieri* arose from the admixture of a population ancestral to
422 present-day western Palearctic populations (86% contribution) and a population closely
423 related to *baueri* North (14%). Additionally, *baueri* North has received 4% ancestry from a
424 population closely related to *taymyrensis* Europe.
425
426 To resolve the nature and relative timing of the admixed origin of *menzbieri* suggested by all
427 previous analyses, we compared the likelihood of alternative scenarios using the approximate
428 Bayesian computation – random forest approach (ABC-RF). In Step 1, we tested whether the
429 apparently clinal variation among the three *baueri* populations was best represented by a
430 simple branching topology or by historical admixture (Figure S4). The best-fitting scenario,
431 representing *baueri* Central as an admixture of *baueri* North and South, received the greatest
432 proportion of RF votes (44.5%), with a posterior probability of 51.0% (Figure S4 and Table
433 S7). This ABC-RF analysis had good power to discriminate among the three scenarios, as
434 suggested by the low prior error rate of 11.4% and the confusion matrix (Table S8).
435 Therefore, we fixed the topology of the main Alaskan branch accordingly in the global
436 scenarios evaluated in Step 2.
437
438 In Step 2 (Figure S5), we compared six possible scenarios for the origin of *menzbieri*: two
439 "null-hypothesis" scenarios in which *menzbieri* simply diverged from one of the two main
440 branches (*a*,*b*), and four in which an admixed *menzbieri* arose at different time points relative
441 to the diversification within each branch (*c*–*f*). The best-supported scenario was *c*, in which
442 the historical admixture occurred prior to the main diversifications within both the western
443 Palearctic and Alaska groups (Figure 4c); this scenario received (mean ± SD) 26.4 ± 0.9% of
444 votes, with a posterior probability of 46.1 ± 2.6% (Figure S5, Table S9). The global prior

error rate of 22.0 ± 0.0% indicated that discriminating power among the six scenarios was good, but with some difficulties in discriminating between scenarios *c* and *e* (Table S10). Scenario *e* was the second best-supported scenario, receiving 25.3 ± 1.0% of votes. This scenario was most similar to *c*, but with the admixture occurring before diversification among *baueri* populations and after *lapponica* diverged from the other western Palearctic populations (Figure 4e).

Each of the 20 demographic parameters of the best-supported scenario was estimated within the ABC-RF framework (Table S11). Timing parameter estimates support the existence of three main lineages at the LGM, with the divergence of the western Palearctic and Alaskan branches occurring c. 38.2K ybp (modal estimate; 5th–95th quantiles: 22.0–93.1K), followed by an admixture giving rise to *menzbieri* c. 22.0K ybp (13.4–52.5K; Figure 5, Table S11). The post-LGM warming period featured *lapponica* diverging from the western Palearctic lineage (c. 16.4K ybp; 9.1–28.9K) and the diversification of *baueri* populations (c. 11.6–12.3K ybp); although we modeled the *baueri* diversification as a divergence followed by an admixture (see Step 1), the two time estimates were essentially indistinguishable, indicating a relatively contemporaneous radiation of three populations, rather than contact after a prolonged isolation (Figure 5). Most recently, the remaining western Palearctic lineage diversified into *taymyrensis* (Europe and Africa) and *yamalensis* populations (c. 4.5–5.2K ybp); these two divergence times were also indistinguishable, rather than clearly sequential (Figure 5).

466 **4 | DISCUSSION**

467

468 **4.1 | Population structure**

469 Previous research showed that the three western Palearctic bar-tailed godwit populations
470 (*lapponica*, *taymyrensis*, and *yamalensis*) were indistinguishable at the mtDNA control
471 region (Bom et al., 2022), consistent with a very recent post-glacial expansion into three
472 breeding areas and migration routes. However, in genome-wide SNPs, we found that
473 *lapponica* was strongly differentiated from *taymyrensis* and *yamalensis*, which were weakly
474 but significantly differentiated from each other (Table 1). This suggests a more complicated
475 phylogeographic history, including a post-LGM colonization by *lapponica* of recently-
476 deglaciated Europe, followed later by emerging structure along two flyways in the source
477 population breeding in the central Russian Arctic. These differences from patterns found in
478 mtDNA illustrate the greater resolution of genome-wide nuclear markers to detect subtle and
479 recent population structure (Edwards & Bensch, 2009).

480

481 We also found unexpected structure among samples collected in the Dutch Wadden Sea
482 during winter, purported to belong to *lapponica*: of these 27 samples, only 6 grouped with the
483 4 individuals sampled in the breeding area of *lapponica*, whereas 19 clearly clustered with
484 *taymyrensis*, and another 2 appeared to represent admixture between the two subspecies
485 (Figure 2). Due to long-term mark-resighting programs on the flyway, we were able to
486 restrict our purported *lapponica* samples to marked individuals that had been observed in
487 multiple years in mid-winter (December–January) in the Wadden Sea and had never been
488 reported in west Africa; this should have provided the best chance to exclude *taymyrensis*
489 individuals from that sample, as *taymyrensis* is expected to pass through western Europe on
490 migration between Russian breeding grounds and non-breeding grounds in west Africa but to

be absent in the winter (Figure 1; Drent & Piersma, 1990; Duijns et al., 2012). Our results strongly indicate that both *taymyrensis* and *lapponica* are present in Europe in the winter.

The currently recognized *lapponica* and *taymyrensis* subspecies were once considered differentially migrating populations of the nominate subspecies *L. l. lapponica*, until the recognition of plumage and morphometric differences between the Fennoscandian and central Russian breeding areas led to the full subspecies status of *taymyrensis* (Engelmoer & Roselaar, 1998); this taxon was itself later split with the recognition of *yamalensis* (Bom et al., 2022). *Lapponica* and *taymyrensis* are generally considered 'leap-frog' migrants, with the entirely of *taymyrensis* wintering in west Africa, south of European-wintering *lapponica* (Figure 1), consistent with historical mark-resight and tracking evidence (Duijns et al., 2012). By contrast, based on morphometric data, Engelmoer (2008) predicted that approximately 20% of bar-tailed godwits wintering in the Dutch Wadden Sea were *taymyrensis*, and thus the migration along the flyway was in fact a 'partial leap-frog system'. Despite this uncertainty, the current population estimate for *lapponica* (150,000–180,000 and increasing; Wetlands International, 2023) is based entirely on winter census data from Europe, assuming no mixing of subspecies. If our results from the Wadden Sea (i.e. c. 70% *taymyrensis*) reflect the subspecies proportions of the entire European wintering population, then the currently accepted population estimate for *lapponica* might overstate the actual population size by a factor of three, and any perceived increase could reflect unknown dynamics in two conflated populations. This should be tested through genetic assignment of a larger and geographically broader sample of the European wintering population, followed by a re-evaluation of the population sizes and conservation status of both *lapponica* and *taymyrensis*.

515 We were unable to completely resolve structure among the three Beringian subspecies due to
516 the small number and high sequencing failure rate of purported *anadyrensis* samples; we thus
517 can conclude little regarding the status or history of that subspecies, which has a distinct
518 migration route through eastern Russia but an incompletely described non-breeding range
519 (Chan et al., 2022; Tomkovich, 2010). However, the three samples in our final data set did
520 not cluster together, grouping with either *menzbieri* (n = 1) or *baueri* (n = 2; Figure 2). This
521 suggests that these individuals, sampled in southeast Chukotka, were most likely passage
522 migrants from the neighboring subspecies to the west and east, rather than from the closest
523 breeding population, but leaves unanswered the question of the potential genetic
524 distinctiveness of *anadyrensis*. Therefore, genetic evaluation of the status of *anadyrensis*
525 awaits analysis of confirmed breeding members of the subspecies.
526
527 Within *baueri*, we confirm that behavioral and morphological differences observed along a
528 latitudinal cline in the Alaska breeding range (Conklin et al., 2010, 2011; Conklin & Battley,
529 2011) are mirrored by a similar genetic cline (Figure 2). Bar-tailed godwits from the entire
530 Alaska breeding range regularly mix at non-breeding sites in New Zealand (Battley et al.,
531 2020; Conklin et al., 2011) and Australia (Wilson et al., 2007) and at migratory staging sites
532 in the Yellow Sea and southwest Alaska (Battley et al., 2012). In the Yellow Sea, many
533 *baueri* individuals also mix freely in staging flocks of *menzbieri* on northward migration (see
534 Figure 1; Battley et al., 2012; Choi et al., 2015). The clear genetic structure maintained
535 among (sub-) populations that regularly meet in the non-breeding season implies that
536 behavioral rigidity, in terms of strict migration timing and fidelity to a breeding region, is
537 sufficient to preclude panmixia among and within subspecies. Within *baueri*, previous
538 research found no clear link between migration timing, which generally follows the
539 latitudinal genetic cline we detected, and variation at the gene Clock, thought to be associated

annual-cycle scheduling in birds (Parody-Merino et al., 2019). Therefore, it remains unclear whether the phenotypic and genetic cline within *baueri* is primarily driven by neutral genetic drift or involves selection, and whether it is emerging or stably maintained over a long time period.

4.2 | Phylogeographic history

Our demographic reconstruction in DIYABC-RF provides the first estimates for divergence times in bar-tailed godwits, and new insights regarding the historical origins of present-day flyway populations. Our divergence time estimate of c. 38K ybp for the two main lineages suggests the ancestors of the western Palearctic and Alaskan populations existed in Siberia and Beringia well before the LGM (Figure 5). This corresponds to a period (c. 40K ybp) when the Bering Sea separated Asia and North America (Farmer et al., 2023) and much of the Chukotka Peninsula was glaciated (Batchelor et al., 2019); either or both of these factors could have caused or perpetuated isolation of the two lineages. We inferred a subsequent admixture of the two lineages c. 22K ybp, giving rise to present-day *menzbieri* (Figure 5). During this period, just prior to and including the LGM, Beringia was largely unglaciated (Batchelor et al., 2019) and lower sea levels created a connection between the continents via the Bering Land Bridge (c. 36–11K ybp; Farmer et al., 2023), a situation that could have created new breeding habitat available for colonization from both the west and the east, or conceivably re-connected breeding populations in a continuous swath of tundra habitat stretching from Chukotka to Alaska. Indeed, reconstructed vegetation histories indicate that at least part of the Bering Land bridge hosted graminoid and herbaceous tundra, the preferred breeding habitat of bar-tailed godwits, during the LGM (Wang et al., 2017). Presumably, subsequent re-flooding of the Bering Strait (by c. 11K ybp) and incremental reduction and isolation of tundra habitat associated with the warming period leading to the mid-Holocene

565 Climatic Optimum (c. 8K ybp; Kraaijeveld & Nieboer, 2000; Stewart & Dalén, 2008;
566 Wauchope et al., 2017) served to isolate these three extant lineages into their present-day
567 breeding ranges (Figure 1); similar structure across Beringia is found in numerous avian taxa
568 (Winker et al., 2023)
569
570 Because significant portions of Alaska have remained unglaciated for hundreds of thousands
571 of years (Batchelor et al., 2019; Winker et al., 2023) and our results suggest no temporal limit
572 to *baueri*'s occupation of its present-day breeding range, we can infer no theoretical
573 maximum age of that population's trans-Pacific migration (Gill et al., 2009). Therefore, we
574 cannot help discern between scenarios of *in situ* evolution of these extremely long non-stop
575 flights in the Pacific versus incremental up-scaling of flight distances through eastward
576 expansion of godwits from Asia (Hedenström, 2010; Piersma et al., 2022). We can only infer
577 that any such eastward expansion did not appear to occur recently (e.g. post-LGM), as *baueri*
578 has apparently existed in Alaska for sufficient time for genetic and morphological structure to
579 develop along a latitudinal cline (Conklin et al., 2011). However, our inference of a radiation
580 into this cline c. 12K ybp is potentially consistent with expansion northward or southward
581 within Alaska, or with emerging isolation-by-distance across a stably occupied area.
582 Paleoclimatic modeling, to assess change in both atmospheric circulation and habitats in the
583 Pacific Basin across time, may reveal more about how long *baueri* could theoretically have
584 been migrating across the Pacific in the current manner (Piersma et al., 2022).
585
586 If bar-tailed godwits existed in a Siberian-Beringian refugium (stretching from the West
587 Siberian Plain to Alaska) at the LGM and then expanded westward with the de-glaciation of
588 Europe (c. 14K ybp), then we would expect *lapponica* to have diverged very recently from
589 other western Palearctic lineages, particularly given the expected delay between geographic

separation and genetic divergence. In this light, our inferred divergence of *lapponica* c. 16K ybp is unexpected, as their present-day breeding range in Fennoscandia was not available until at least 3,000 years after that (Stroeven et al., 2016). This divergence-time estimate is not easily explained by a simple westward expansion, and favors a scenario of isolation followed by expansion from tundra breeding areas that were available south or southeast of glaciated Europe during or soon after the LGM. In fact, such refugia, including in central/southern Europe, have been inferred for tundra-breeding shorebirds (Arcones et al., 2021) and other taxa (Hewitt, 2004; Sommer & Nadachowski, 2006; Taberlet et al., 1998). If the breeding grounds of *lapponica* gradually moved toward Fennoscandia from central Europe as glaciers retreated north, then its present-day migration route would re-trace that northward expansion, as has been hypothesized for numerous migratory birds that either originally evolved from sedentary populations (Rappole & Jones, 2002; Salewski & Bruderer, 2007) or oscillated between short- and long-distance migration as northern areas were impacted by cyclic glaciations (Bruderer & Salewski, 2008; Zink & Gardner, 2017).

At the LGM, the lineage that recently gave rise to *taymyrensis* and *yamalensis* could have existed east or south of the glaciers that extended from Europe to the Taimyr Peninsula of central Russia (Arcones et al., 2021; Batchelor et al., 2019). We may then expect that the present-day breeding range and migration of *yamalensis* (Figure 1) would most closely resemble the state of the western Palearctic lineage at the LGM. Consistent with this, there is evidence of tundra habitats existing south of the ice-dammed West Siberian Lake at the LGM (Binney et al., 2017; Mangerud et al., 2004), close to the present-day breeding area of *yamalensis* in the West Siberian Plain. Currently, *taymyrensis* and *yamalensis* have some degree of isolation in breeding areas along a latitudinal and longitudinal gradient (Figure 1; Bom et al., 2022). This may suggest that a northeastward expansion of breeding range toward

615 the Taimyr Peninsula was associated with discovery of the migration route of *taymyrensis*
616 through western Europe (Figure 1) after glaciers retreated.
617
618 We have presented the first unequivocal evidence that *taymyrensis* can be found in Europe in
619 winter, and it is therefore unclear whether this is a new, perhaps emerging, development in
620 modern times (i.e. tens or hundreds of years) or a stable situation that went previously
621 undetected. However, the detection of two apparent F1 *lapponica*/*taymyrensis* hybrids (see
622 Figure 2) in our relatively small sample from the Wadden Sea appears more indicative of a
623 brief period of significant contact between the subspecies. Also, the negligible differentiation
624 between European- and Africa-wintering *taymyrensis* (F_{ST} = 0.001) provides no evidence of
625 further structure within that subspecies. Taken together, our results suggest that the existence
626 of *taymyrensis* in Europe, or at least conditions promoting successful cross-population
627 recruitment, is a recent or increasing phenomenon.
628
629 **4.3 | Population structure in long-distance migrants**
630 Highly mobile organisms, such as migratory birds, are interesting cases for studying the
631 effects of spatial isolation on population structure. On one hand, highly mobile species are
632 expected to have high dispersal ability, which should decrease the strength of physical or
633 ecological barriers to gene flow, resulting in shallow structure, or even panmixia, across large
634 geographic areas. Accordingly, a negative relationship between dispersal ability and
635 population structure has been demonstrated in various taxa (Bohonak, 1999; Medina et al.,
636 2018). In birds, both migratory tendency and flight capacity *per se* have been linked with
637 increased dispersal and decreased population structure and speciation (Arguedas & Parker,
638 2000; Claramunt et al., 2012). By this reasoning, we should expect unimpeded gene flow in
639 an extreme long-distance migrant like the bar-tailed godwit, which can fly distances >11,000

640 km across formidable ecological barriers without resting, eating, or drinking (Gill et al.,
641 2009; Piersma et al., 2022), predicting negligible sub-specific population genetic structure.
642
643 Paradoxically, migration has also been linked with increased rates of speciation and
644 diversification in birds (Rolland et al., 2014; Winger et al., 2014). Long-distance migration is
645 associated with high site-fidelity and rigid behavioral and physiological traits that enable
646 timely exploitation of predictable seasonal resources across hemispheres (Åkesson et al.,
647 2017; Conklin et al., 2013; Winger et al., 2019). These traits predict low effective dispersal
648 among neighboring populations, either through strict spatial or temporal isolation, or by
649 preventing successful recruitment by immigrants (Nosil et al., 2005). In this light, we might
650 expect bar-tailed godwits to exhibit strong structure among flyway populations.
651
652 Within this species, we see evidence for both ends of the continuum: in the west, negligible
653 structure between two populations with adjacent breeding areas but separate ranges in the
654 non-breeding season (*taymyrensis* and *yamalensis*), and in the east, clinal structure within a
655 single subspecies, where individuals freely mix throughout the non-breeding season (*baueri*).
656 The latter situation, involving birds making the longest non-stop migratory flights on earth,
657 demonstrates the weak link between dispersal *ability* (in terms of flight capacity) and actual
658 dispersal. In fact, bar-tailed godwits are known for extremely rigid site-fidelity at non-
659 breeding and migratory staging sites (Conklin et al., 2013; Rakhimberdiev et al., 2018), and
660 are presumed to show similar fidelity to breeding sites as adults. The very fine-scale structure
661 we demonstrate within the Alaska breeding range suggests that natal dispersal is also quite
662 restricted in *baueri* (i.e. relative to distances of c. 400–800 km between our sampling sites;
663 Figure 1). As we have no reason to expect weaker site-fidelity in other bar-tailed godwit
664 populations, we presume the weak differentiation between *taymyrensis* and *yamalensis*,

665 which may meet at pre- and post-breeding areas and breed <500 km from each other (Bom et
666 al., 2022), is a result of their recent divergence (c. 6,000 ybp) rather than high levels of gene
667 flow.
668
669 While not clearly related to dispersal and gene flow, flight capacity may be more indicative
670 of a species' propensity for exploration and colonization of new migratory flyways. As
671 illustrated in other long-distance migratory shorebirds, such as dunlin, *Calidris alpina*
672 (Wenink et al., 1996), and red knot, *C. canutus* (Conklin et al., 2022), such species appear to
673 respond relatively quickly to major climatic changes, such as retreat of glacial ice sheets,
674 with establishment of new flyway populations (as we have demonstrated with the *lapponica*
675 subspecies). As migration of adult birds tends to be more conservative, such 'innovations' in
676 a population may result largely from inexperienced juveniles conducting their first migration
677 (Cresswell, 2014; Verhoeven et al., 2022). Intriguingly, bar-tailed godwits and other long-
678 distance migrants also seem flexible (at least in evolutionary timescales) with regard to
679 migration distance. For example, *lapponica* and *yamalensis*, among the youngest of bar-tailed
680 godwit subspecies, migrate as little as 2,500–5,000 km between breeding and non-breeding
681 grounds, whereas the other four subspecies travel one-way distances of 10,000–18,000 km
682 (Figure 1). This shows that behavioral and physiological 'upscaling' to accommodate the
683 world's longest flights (Hedenström, 2010) is not a one-way journey; it may be reversed,
684 with regression toward short-distance migration, if the ecological opportunity arises.

ACKNOWLEDGEMENTS

We thank Per Palsbøll and Ritsert Jansen for guidance and help to develop the funding proposal, and to members of the Palsbøll and Fontaine laboratories at the University of Groningen and Montpellier for helpful discussions during project conception and analysis, respectively. We thank Anneke Bol at NIOZ Royal Netherlands Institute for Sea Research for DNA extractions of Mauritania samples; Marco van der Velde for laboratory assistance in Groningen; Eric Johnson and Paul Etter (SNPsaurus) for sequencing, bioinformatics, and technical expertise; and the Centre for Information Technology of the University of Groningen (particularly Bob Dröge and Cristian Marocico) for technical support and access to the Peregrine high-performance computing cluster. For providing samples, we thank Massey University, Moscow Lomonosov State University Zoological Museum, NIOZ, Royal Ontario Museum (Oliver Haddrath and Mark Peck), U.S. Geological Survey Alaska Science Center, University of Groningen, and University of Washington Burke Museum. For godwit capture and field sampling, we thank Luke DeCicco, Jimmy de Fouw, Maks Dementyev, Nick Hajdukovich, Jim Johnson, Murray Potter, Adrian Riegen, David Melville, Dan Mulcahy, Adrian Riegen, Rob Schuckard, Craig Steed, and Cleland Wallace, plus numerous local volunteers. In Australia, we thank Broome Bird Observatory and the Australasian Wader Studies Group for logistical and field work support, and we acknowledge the Yawuru People via the offices of Nyamba Buru Yawuru Limited for permission to capture godwits on the shores of Roebuck Bay, traditional lands of the Yawuru people. Sampling was supported by the David and Lucile Packard Foundation (Alaska, Australia, and New Zealand), BirdLife Netherlands and WWF-Netherlands (Australia), and a Royal Society of New Zealand Marsden Fund grant to P.F.B. and Andrew Fidler (New Zealand). The Prins Bernhard Cultuurfonds grant to T.P. started up the long-term efforts in Mauritania, supported now by

operational grants from NIOZ; we thank the authorities of the Parc National du Banc d'Arguin for access and support. Work in the Wadden Sea was supported by Waddenfonds (project Metawad, WF209925) and operational funding from NIOZ. Work in Oman was financially supported by the Research Council (TRC) of the Sultanate of Oman (ORG/EBR/12/002). The core of this project was supported by a Dutch Research Council (NWO) grant to T.P. (ALW-Open Programme grant, 'Ecological drivers of global flyway evolution' 824.01.001). Any use of trade, product or firm names is for descriptive purposes only and does not imply endorsement by the U.S. Government.

AUTHOR CONTRIBUTIONS

J.R.C., Y.I.V., M.C.F. and T.P. conceived and designed the study. P.F.B., R.A.B., R.E.G., C.J.H., J.t.H., D.R.R., T.L.T., N.W., and P.S.T. organized and performed field sampling and/or maintained individual resight-history databases. J.R.C. and Y.I.V. curated samples and conducted the labwork. J.R.C., M.J.M.L. and M.C.F. analysed and interpreted the data, with assistance from Y.I.V. J.R.C. and M.C.F. wrote the manuscript, with major contributions from Y.I.V. and T.P. All authors provided feedback and helped edit the manuscript.

DATA AVAILABILITY STATEMENT

Demultiplexed nextRAD short-read data were deposited in NCBI's SRA archives under BioProject ID xxx (TBA). Associated files (VCF and metadata) were deposited in DRYAD (doi: TBA).

BENEFIT-SHARING STATEMENT

All genetic samples were collected with collaboration and/or consultation with local communities, and all principal collaborators who provided samples are included as co-authors. The research addresses an international priority concern, which is the conservation of the study organism. Benefits from this research accrue from the sharing of our data and results with the scientific and stakeholder communities, both directly and on public databases as described above.

REFERENCES

Åkesson, S., & Helm, B. (2020). Endogenous programs and flexibility in bird migration. *Frontiers in Ecology and Evolution*, *8*(March), 1–20. https://doi.org/10.3389/fevo.2020.00078

Åkesson, S., Ilieva, M., Karagicheva, J., Rakhimberdiev, E., Tomotani, B., & Helm, B. (2017). Timing avian long-distance migration: From internal clock mechanisms to global flights. *Philosophical Transactions of the Royal Society B: Biological Sciences*, *372*(1734). https://doi.org/10.1098/rstb.2016.0252

Alerstam, T., Hedenstrom, A., & Akesson, S. (2003). Long-distance migration: evolution and determinants. *Oikos*, *103*(2), 247–260. https://doi.org/10.1034/j.1600-0706.2003.12559.x

Alexander, D. H., & Lange, K. (2011). Enhancements to the ADMIXTURE algorithm for individual ancestry estimation. *BMC Bioinformatics*, *12*, 246. https://doi.org/10.1186/1471-2105-12-246

Alexander, D. H., Novembre, J., & Lange, K. (2009). Fast model-based estimation of ancestry in unrelated individuals. *Genome Research*, *19*, 1655–1664. https://doi.org/10.1101/gr.094052.109.vidual

Anderson, E. C., & Dunham, K. K. (2008). The influence of family groups on inferences made with the program Structure. *Molecular Ecology Resources*, *8*(6), 1219–1229. https://doi.org/10.1111/j.1755-0998.2008.02355.x

Archer, F. I., Adams, P. E., & Schneiders, B. B. (2017). *strataG*: An R package for manipulating, summarizing and analysing population genetic data. *Molecular Ecology Resources*, *17*(1), 5–11. https://doi.org/10.1111/1755-0998.12559

Arcones, A., Ponti, R., Ferrer, X., & Vieites, D. R. (2021). Pleistocene glacial cycles as drivers of allopatric differentiation in Arctic shorebirds. *Journal of Biogeography*, *48*(4), 747–759. https://doi.org/10.1111/jbi.14023

Arguedas, N., & Parker, P. (2000). Seasonal migration and genetic population structure in House Wrens. *Condor*, *102*(3), 517–528.

Avise, J. C. (2009). Phylogeography: Retrospect and prospect. *Journal of Biogeography*, *36*(1), 3–15. https://doi.org/10.1111/j.1365-2699.2008.02032.x

Avise, J. C., & Walker, D. (1998). Pleistocene phylogeographic effects on avian populations and the speciation process. *Proceedings of the Royal Society B: Biological Sciences*, *265*, 457–463.

Batchelor, C. L., Margold, M., Krapp, M., Murton, D. K., Dalton, A. S., Gibbard, P. L., Stokes, C. R., Murton, J. B., & Manica, A. (2019). The configuration of Northern Hemisphere ice sheets through the Quaternary. *Nature Communications*, *10*(1), 3713. https://doi.org/10.1038/s41467-019-11601-2

Battley, P. F., Conklin, J. R., Parody-Merino, Á. M., Langlands, P. A., Southey, I., Burns, T., Melville, D. S., Schuckard, R., Riegen, A. C., & Potter, M. A. (2020). Interacting roles of breeding geography and early-life settlement in godwit migration timing. *Frontiers in Ecology and Evolution*, *8*, 52. https://doi.org/10.3389/fevo.2020.00052

Battley, P. F., Warnock, N., Tibbitts, T. L., Gill, R. E., Piersma, T., Hassell, C. J., Douglas, D. C., Mulcahy, D. M., Gartrell, B. D., Schuckard, R., Melville, D. S., & Riegen, A. C. (2012). Contrasting extreme long-distance migration patterns in bar-tailed godwits *Limosa lapponica*. *Journal of Avian Biology*, *43*(1), 21–32. https://doi.org/10.1111/j.1600-048X.2011.05473.x

Beaumont, M. A., Zhang, W., & Balding, D. J. (2002). Approximate Bayesian computation in population genetics. *Genetics*, *162*(4), 2025–2035.

Binney, H., Edwards, M., Macias-Fauria, M., Lozhkin, A., Anderson, P., Kaplan, J. O., Andreev, A., Bezrukova, E., Blyakharchuk, T., Jankovska, V., Khazina, I., Krivonogov, S., Kremenetski, K., Nield, J., Novenko, E., Ryabogina, N., Solovieva, N., Willis, K., & Zernitskaya, V. (2017). Vegetation of Eurasia from the last glacial maximum to present: Key biogeographic patterns. *Quaternary Science Reviews*, *157*, 80–97.

https://doi.org/10.1016/j.quascirev.2016.11.022

BirdLife International. (2023). *Bar-tailed Godwit Limosa lapponica*. http://datazone.birdlife.org/

Bohonak, A. J. (1999). Dispersal, gene flow, and population structure. *Quarterly Review of Biology*, *74*(1), 21–45.

Bom, R. A., Conklin, J. R., Verkuil, Y. I., Alves, J. A., de Fouw, J., Dekinga, A., Hassell, C. J., Klaassen, R. H. G., Kwarteng, A. Y., Rakhimberdiev, E., Rocha, A., ten Horn, J., Tibbitts, T. L., Tomkovich, P. S., Victor, R., & Piersma, T. (2022). Central-West Siberian-breeding Bar-tailed Godwits (*Limosa lapponica*) segregate in two morphologically distinct flyway populations. *Ibis*, *164*(2), 468–485. https://doi.org/10.1111/ibi.13024

Bruderer, B., & Salewski, V. (2008). Evolution of bird migration in a biogeographical context. *Journal of Biogeography*, *35*(11), 1951–1959. https://doi.org/10.1111/j.1365-2699.2008.01992.x

Bushnell, B. (2016). *BBMap*. University of California. http://sourceforge.net/projects/bbmap

Chan, Y. C., Tibbitts, T. L., Dorofeev, D., Hassell, C. J., & Piersma, T. (2022). Hidden in plain sight: migration routes of the elusive Anadyr bar-tailed godwit revealed by satellite tracking. *Journal of Avian Biology*, *2022*(8), e02988. https://doi.org/10.1111/jav.02988

Chang, C. C., Chow, C. C., Tellier, L. C. A. M., Vattikuti, S., Purcell, S. M., & Lee, J. J. (2015). Second-generation PLINK: Rising to the challenge of larger and richer datasets. *GigaScience*, *4*(1), 1–16. https://doi.org/10.1186/s13742-015-0047-8

Choi, C. Y., Battley, P. F., Potter, M. A., Rogers, K. G., & Ma, Z. (2015). The importance of Yalu Jiang coastal wetland in the north Yellow Sea to Bar-tailed Godwits *Limosa lapponica* and Great Knots *Calidris tenuirostris* during northward migration. *Bird Conservation International*, *25*(1), 53–70. https://doi.org/10.1017/S0959270914000124

Choisy, M., Franck, P., & Cornuet, J. M. (2004). Estimating admixture proportions with microsatellites: Comparison of methods based on simulated data. *Molecular Ecology*, *13*(4), 955–968. https://doi.org/10.1111/j.1365-294X.2004.02107.x

Claramunt, S., Derryberry, E. P., Remsen, J. V., & Brumfield, R. T. (2012). High dispersal ability inhibits speciation in a continental radiation of passerine birds. *Proceedings of the Royal Society B: Biological Sciences*, *279*(1733), 1567–1574. https://doi.org/10.1098/rspb.2011.1922

Collin, F. D., Durif, G., Raynal, L., Lombaert, E., Gautier, M., Vitalis, R., Marin, J. M., &

Estoup, A. (2021). Extending approximate Bayesian computation with supervised machine learning to infer demographic history from genetic polymorphisms using DIYABC Random Forest. *Molecular Ecology Resources*, *21*(8), 2598–2613. https://doi.org/10.1111/1755-0998.13413

Conklin, J. R., & Battley, P. F. (2011). Contour-feather moult of Bar-tailed Godwits (*Limosa lapponica baueri*) in New Zealand and the Northern Hemisphere reveals multiple strategies by sex and breeding region. *Emu*, *111*(4), 330–340. https://doi.org/10.1071/MU11011

Conklin, J. R., Battley, P. F., & Potter, M. A. (2013). Absolute consistency: Individual versus population variation in annual-cycle schedules of a long-distance migrant bird. *PLoS ONE*, *8*(1), e54535. https://doi.org/10.1371/journal.pone.0054535

Conklin, J. R., Battley, P. F., Potter, M. A., & Fox, J. W. (2010). Breeding latitude drives individual schedules in a trans-hemispheric migrant bird. *Nature Communications*, *1*(5), ncomms1072. https://doi.org/10.1038/ncomms1072

Conklin, J. R., Battley, P. F., Potter, M. A., & Ruthrauff, D. R. (2011). Geographic variation in morphology of Alaska-breeding bar-tailed godwits (*Limosa lapponica*) is not maintained on their nonbreeding grounds in New Zealand. *Auk*, *128*(2), 363–373. https://doi.org/10.1525/auk.2011.10231

Conklin, J. R., Senner, N. R., Battley, P. F., & Piersma, T. (2017). Extreme migration and the individual quality spectrum. *Journal of Avian Biology*, *48*(1), 19–36. https://doi.org/10.1111/jav.01316

Conklin, J. R., Verkuil, Y. I., Battley, P. F., Hassell, C. J., ten Horn, J., Johnson, J. A., Tomkovich, P. S., Baker, A. J., Piersma, T., & Fontaine, M. C. (2022). Global flyway evolution in red knots *Calidris canutus* and genetic evidence for a Nearctic refugium. *Molecular Ecology*, *31*(7), 2124–2139. https://doi.org/10.1111/mec.16379

Cresswell, W. (2014). Migratory connectivity of Palaearctic-African migratory birds and their responses to environmental change: The serial residency hypothesis. *Ibis*, *156*(3), 493–510. https://doi.org/10.1111/ibi.12168

Danecek, P., Auton, A., Abecasis, G., Albers, C. A., Banks, E., DePristo, M. A., Handsaker, R. E., Lunter, G., Marth, G. T., Sherry, S. T., McVean, G., & Durbin, R. (2011). The variant call format and VCFtools. *Bioinformatics*, *27*(15), 2156–2158. https://doi.org/10.1093/bioinformatics/btr330

Drent, R., & Piersma, T. (1990). An exploration of the energetics of leap-frog migration in

arctic breeding waders. In E. Gwinner (Ed.), *Bird migration: the physiology and ecophysiology* (pp. 399–412). https://doi.org/10.1007/978-3-642-74542-3

Duijns, S., Jukema, J., Spaans, B., van Horssen, P., & Piersma, T. (2012). Revisiting the proposed leap-frog migration of Bar-tailed Godwits along the East-Atlantic Flyway. *Ardea*, *100*(1), 37–43. https://doi.org/10.5253/078.100.0107

Edwards, S., & Bensch, S. (2009). Looking forwards or looking backwards in avian phylogeography? A comment on Zink and Barrowclough 2008. *Molecular Ecology*, *18*(14), 2930–2933. https://doi.org/10.1111/j.1365-294X.2009.04270.x

Ehlers, J., & Gibbard, P. L. (2007). The extent and chronology of Cenozoic Global Glaciation. *Quaternary International*, *164–165*, 6–20. https://doi.org/10.1016/j.quaint.2006.10.008

Engelmoer, M. (2008). *Breeding origins of wader populations utilizing the Dutch Wadden Sea as deduced from body dimensions, body mass and primary moult*. University of Groningen.

Engelmoer, M., & Roselaar, C. S. (1998). *Geographical variation in waders*. Kluwer Academic Publishers.

Estoup, A., Lombaert, E., Marin, J.-M., Guillemaud, T., Pudlo, P., Robert, C. P., & Cornuet, J.-M. (2012). Estimation of demo-genetic model probabilities with Approximate Bayesian Computation using linear discriminant analysis on summary statistics. *Molecular Ecology Resources*, *12*(5), 846–855. https://doi.org/10.1111/j.1755-0998.2012.03153.x

Farmer, J. R., Pico, T., Underwood, O. M., Cleveland Stout, R., Granger, J., Cronin, T. M., Fripiat, F., Martínez-García, A., Haug, G. H., & Sigman, D. M. (2023). The Bering Strait was flooded 10,000 years before the Last Glacial Maximum. *Proceedings of the National Academy of Sciences*, *120*(1), e2206742119. https://doi.org/10.1073/pnas

Gill, Jr., R. E., Douglas, D. C., Handel, C. M., Tibbitts, T. L., Hufford, G., & Piersma, T. (2014). Hemispheric-scale wind selection facilitates bar-tailed godwit circum-migration of the Pacific. *Animal Behaviour*, *90*, 117–130. https://doi.org/10.1016/j.anbehav.2014.01.020

Gill, Jr., R. E., Tibbitts, T. L., Douglas, D. C., Handel, C. M., Mulcahy, D. M., Gottschalck, J. C., Warnock, N., McCaffery, B. J., Battley, P. F., & Piersma, T. (2009). Extreme endurance flights by landbirds crossing the Pacific Ocean: ecological corridor rather than barrier? *Proceedings of the Royal Society B: Biological Sciences*, *276*(1656), 447–

457. https://doi.org/10.1098/rspb.2008.1142

Hedenström, A. (2010). Extreme endurance migration: What is the limit to non-stop flight? *PLoS Biology*, *8*(5), 1–6. https://doi.org/10.1371/journal.pbio.1000362

Hewitt, G. M. (2000). The genetic legacy of the Quarternary ice ages. *Nature*, *405*, 907–913. https://doi.org/10.1038/35016000

Hewitt, G. M. (2004). Genetic consequences of climatic oscillations in the Quaternary. *Philosophical Transactions of the Royal Society B: Biological Sciences*, *359*(1442), 183–195. https://doi.org/10.1098/rstb.2003.1388

Hivert, V., Leblois, R., Petit, E. J., Gautier, M., & Vitalis, R. (2018). Measuring genetic differentiation from Pool-seq data. *Genetics*, *210*(1), 315–330. https://doi.org/10.1534/genetics.118.300900

Kamvar, Z. N., Tabima, J. F., & Grünwald, N. J. (2014). Poppr: an R package for genetic analysis of populations with clonal, partially clonal, and/or sexual reproduction. *PeerJ*, *2*, e281. https://doi.org/10.7717/peerj.281

Keenan, K., McGinnity, P., Cross, T. F., Crozier, W. W., & Prodöhl, P. A. (2013). DiveRsity: An R package for the estimation and exploration of population genetics parameters and their associated errors. *Methods in Ecology and Evolution*, *4*(8), 782–788. https://doi.org/10.1111/2041-210X.12067

Knowles, L. L., & Maddison, W. P. (2002). Statistical phylogeography. *Molecular Ecology*, *11*(12), 2623–2635. https://doi.org/10.1046/j.1365-294X.2002.01637.x

Kopelman, N. M., Mayzel, J., Jakobsson, M., Rosenberg, N. A., & Mayrose, I. (2015). Clumpak: A program for identifying clustering modes and packaging population structure inferences across *K*. *Molecular Ecology Resources*, *15*(5), 1179–1191. https://doi.org/10.1111/1755-0998.12387

Kraaijeveld, K., & Nieboer, E. N. (2000). Late Quaternary paleogeography and evolution of arctic breeding waders. *Ardea*, *88*(2), 193–205.

Kubelka, V., Sandercock, B. K., Székely, T., & Freckleton, R. P. (2022). Animal migration to northern latitudes: environmental changes and increasing threats. *Trends in Ecology and Evolution*, *37*(1), 30–41. https://doi.org/10.1016/j.tree.2021.08.010

Leppälä, K., Nielsen, S. V., & Mailund, T. (2017). admixturegraph: An R package for admixture graph manipulation and fitting. *Bioinformatics*, *33*(11), 1738–1740. https://doi.org/10.1093/bioinformatics/btx048

Lischer, H. E. L., & Excoffier, L. (2012). PGDSpider: An automated data conversion tool for

connecting population genetics and genomics programs. *Bioinformatics*, *28*(2), 298–299. https://doi.org/10.1093/bioinformatics/btr642

Maier, R., Flegontov, P., Flegontova, O., Işıldak, U., & Changmai, P. (2023). On the limits of fitting complex models of population history to *f*-statistics. *ELife*, *12*, e85492.

Mangerud, J., Jakobsson, M., Alexanderson, H., Astakhov, V., Clarke, G. K. C., Henriksen, M., Hjort, C., Krinner, G., Lunkka, J. P., Möller, P., Murray, A., Nikolskaya, O., Saarnisto, M., & Svendsen, J. I. (2004). Ice-dammed lakes and rerouting of the drainage of northern Eurasia during the Last Glaciation. *Quaternary Science Reviews*, *23*(11–13), 1313–1332. https://doi.org/10.1016/j.quascirev.2003.12.009

Medina, I., Cooke, G. M., & Ord, T. J. (2018). Walk, swim or fly? Locomotor mode predicts genetic differentiation in vertebrates. *Ecology Letters*, *21*(5), 638–645. https://doi.org/10.1111/ele.12930

Méndez, V., Alves, J. A., Gill, J. A., & Gunnarsson, T. G. (2018). Patterns and processes in shorebird survival rates: a global review. *Ibis*, *160*(4), 723–741. https://doi.org/10.1111/ibi.12586

Milá, B., Smith, T. B., & Wayne, R. K. (2006). Postglacial population expansion drives the evolution of long-distance migration in a songbird. *Evolution*, *60*(11), 2403–2409. https://doi.org/10.1111/j.0014-3820.2006.tb01875.x

Nei, M. (1972). Genetic distance between populations. *American Naturalist*, *106*(949), 283–292.

Nosil, P., Vines, T. H., & Funk, D. J. (2005). Perspective: Reproductive isolation caused by natural selection against immigrants from divergent habitats. *Evolution*, *59*(4), 705–719. https://doi.org/10.1554/04-428

Paradis, E., & Schliep, K. (2019). ape 5.0: An environment for modern phylogenetics and evolutionary analyses in R. *Bioinformatics*, *35*(3), 526–528. https://doi.org/10.1093/bioinformatics/bty633

Parody-Merino, Á. M., Battley, P. F., Conklin, J. R., & Fidler, A. E. (2019). No evidence for an association between *Clock* gene allelic variation and migration timing in a long-distance migratory shorebird (*Limosa lapponica baueri*). *Oecologia*, *191*(4), 843–859. https://doi.org/10.1007/s00442-019-04524-8

Patterson, N., Moorjani, P., Luo, Y., Mallick, S., Rohland, N., Zhan, Y., Genschoreck, T., Webster, T., & Reich, D. (2012). Ancient admixture in human history. *Genetics*, *192*(3), 1065–1093. https://doi.org/10.1534/genetics.112.145037

Patterson, N., Price, A. L., & Reich, D. (2006). Population structure and eigenanalysis. *PLoS Genetics*, *2*(12), 2074–2093. https://doi.org/10.1371/journal.pgen.0020190

Pielou, E. C. (1991). *After the Ice Age: The Return of Life to Glaciated North America*. University of Chicago Press.

Piersma, T., Gill, Jr., R. E., Ruthrauff, D. R., Guglielmo, C. G., Conklin, J. R., & Handel, C. M. (2022). The Pacific as the world's greatest theater of bird migration: Extreme flights spark questions about physiological capabilities, behavior, and the evolution of migratory pathways. *Ornithology*, *139*(2), ukab086. https://doi.org/10.1093/ornithology/ukab086

Piersma, T., Pérez-Tris, J., Mouritsen, H., Bauchinger, U., & Bairlein, F. (2005). Is there a "migratory syndrome" common to all migrant birds? *Annals of the New York Academy of Sciences*, *1046*, 282–293. https://doi.org/10.1196/annals.1343.026

Pudlo, P., Marin, J. M., Estoup, A., Cornuet, J. M., Gautier, M., & Robert, C. P. (2016). Reliable ABC model choice via random forests. *Bioinformatics*, *32*(6), 859–866. https://doi.org/10.1093/bioinformatics/btv684

Rakhimberdiev, E., Duijns, S., Karagicheva, J., Camphuysen, C. J., VRS Castricum, Dekinga, A., Dekker, R., Gavrilov, A., ten Horn, J., Jukema, J., Saveliev, A., Soloviev, M., Tibbitts, T. L., van Gils, J. A., & Piersma, T. (2018). Fuelling conditions at staging sites can mitigate Arctic warming effects in a migratory bird. *Nature Communications*, *9*(1), 4263. https://doi.org/10.1038/s41467-018-06673-5

Rappole, J. H., & Jones, P. (2002). Evolution of old and new world migration systems. *Ardea*, *90*(3), 525–537.

Raynal, L., Marin, J. M., Pudlo, P., Ribatet, M., Robert, C. P., & Estoup, A. (2019). ABC random forests for Bayesian parameter inference. *Bioinformatics*, *35*(10), 1720–1728. https://doi.org/10.1093/bioinformatics/bty867

Reich, D., Thangaraj, K., Patterson, N., Price, A. L., & Singh, L. (2009). Reconstructing Indian population history. *Nature*, *461*(7263), 489–494. https://doi.org/10.1038/nature08365

Robinson, R. A., Crick, H. Q. P., Learmonth, J. A., Maclean, I. M. D., Thomas, C. D., Bairlein, F., Forchhammer, M. C., Francis, C. M., Gill, J. A., Godley, B. J., Harwood, J., Hays, G. C., Huntley, B., Hutson, A. M., Pierce, G. J., Rehfisch, M. M., Sims, D. W., Begoña Santos, M., Sparks, T. H., … Visser, M. E. (2009). Travelling through a warming world: Climate change and migratory species. *Endangered Species Research*,

7(2), 87–99. https://doi.org/10.3354/esr00095

Rodríguez-Ramilo, S. T., & Wang, J. (2012). The effect of close relatives on unsupervised Bayesian clustering algorithms in population genetic structure analysis. *Molecular Ecology Resources*, *12*(5), 873–884. https://doi.org/10.1111/j.1755-0998.2012.03156.x

Rolland, J., Jiguet, F., Jønsson, K. A., Condamine, F. L., & Morlon, H. (2014). Settling down of seasonal migrants promotes bird diversification. *Proceedings of the Royal Society B: Biological Sciences*, *281*(1784). https://doi.org/10.1098/rspb.2014.0473

Russello, M. A., Waterhouse, M. D., Etter, P. D., & Johnson, E. A. (2015). From promise to practice: pairing non-invasive sampling with genomics in conservation. *PeerJ*, *3*, e1106. https://doi.org/10.7717/peerj.1106

Salewski, V., & Bruderer, B. (2007). The evolution of bird migration – A synthesis. *Naturwissenschaften*, *94*(4), 268–279. https://doi.org/10.1007/s00114-006-0186-y

Sommer, R. S., & Nadachowski, A. (2006). Glacial refugia of mammals in Europe: Evidence from fossil records. *Mammal Review*, *36*(4), 251–265. https://doi.org/10.1111/j.1365-2907.2006.00093.x

Stewart, J. R., & Dalén, L. (2008). Is the glacial refugium concept relevant for northern species? A comment on Pruett and Winker 2005. *Climatic Change*, *86*, 19–22. https://doi.org/10.1007/s10584-007-9366-9

Stroeven, A. P., Hättestrand, C., Kleman, J., Heyman, J., Fabel, D., Fredin, O., Goodfellow, B. W., Harbor, J. M., Jansen, J. D., Olsen, L., Caffee, M. W., Fink, D., Lundqvist, J., Rosqvist, G. C., Strömberg, B., & Jansson, K. N. (2016). Deglaciation of Fennoscandia. *Quaternary Science Reviews*, *147*, 91–121. https://doi.org/10.1016/j.quascirev.2015.09.016

Studds, C. E., Kendall, B. E., Murray, N. J., Wilson, H. B., Rogers, D. I., Clemens, R. S., Gosbell, K., Hassell, C. J., Jessop, R., Melville, D. S., Milton, D. A., Minton, C. D. T., Possingham, H. P., Riegen, A. C., Straw, P., Woehler, E. J., & Fuller, R. A. (2017). Rapid population decline in migratory shorebirds relying on Yellow Sea tidal mudflats as stopover sites. *Nature Communications*, *8*, 14895. https://doi.org/10.1038/ncomms14895

Taberlet, P., Fumagalli, L., Wust-Saucy, A. G., & Cosson, J. F. (1998). Comparative phylogeography and postglacial colonization routes in Europe. *Molecular Ecology*, *7*(4), 453–464. https://doi.org/10.1046/j.1365-294x.1998.00289.x

Tan, H. Z., Jansen, J. J. F. J., Allport, G. A., Garg, K. M., Chattopadhyay, B., Irestedt, M.,

Pang, S. E. H., Chilton, G., Gwee, C. Y., & Rheindt, F. E. (2023). Megafaunal extinctions, not climate change, may explain Holocene genetic diversity declines in *Numenius* shorebirds. *ELife*, *12*, e85422.

Tomkovich, P. S. (2010). Assessment of the Anadyr Lowland subspecies of Bar-tailed Godwit *Limosa lapponica anadyrensis*. *Bulletin of the British Ornithologists' Club*, *130*(2), 88–95.

Verhoeven, M. A., Loonstra, A. H. J., McBride, A. D., Kaspersma, W., Hooijmeijer, J. C. E. W., Both, C., Senner, N. R., & Piersma, T. (2022). Age-dependent timing and routes demonstrate developmental plasticity in a long-distance migratory bird. *Journal of Animal Ecology*, *91*(3), 566–579. https://doi.org/10.1111/1365-2656.13641

Wang, Y., Heintzman, P. D., Newsom, L., Bigelow, N. H., Wooller, M. J., Shapiro, B., & Williams, J. W. (2017). The southern coastal Beringian land bridge: cryptic refugium or pseudorefugium for woody plants during the Last Glacial Maximum? *Journal of Biogeography*, *44*(7), 1559–1571. https://doi.org/10.1111/jbi.13010

Wauchope, H. S., Shaw, J. D., Varpe, Ø., Lappo, E. G., Boertmann, D., Lanctot, R. B., & Fuller, R. A. (2017). Rapid climate-driven loss of breeding habitat for Arctic migratory birds. *Global Change Biology*, *23*(3), 1085–1094. https://doi.org/10.1111/gcb.13404

Weir, B. S., & Cockerham, C. C. (1984). Estimating *F*-statistics for the analysis of population structure. *Evolution*, *38*(6), 1358–1370. https://doi.org/10.2307/2409936

Weir, B. S., & Goudet, J. (2017). A unified characterization of population structure and relatedness. *Genetics*, *206*(August), 2085–2103.

Wenink, P. W., Baker, A. J., Rösner, H. U., & Tilanus, M. G. (1996). Global mitochondrial DNA phylogeography of holarctic breeding dunlins (*Calidris alpina*). *Evolution*, *50*(1), 318–330.

Wetlands International. (2023). *Waterbird Population Estimates*. wpe.wetlands.org

Wilson, J. R., Nebel, S., & Minton, C. D. T. (2007). Migration ecology and morphometrics of two Bar-tailed Godwit populations in Australia. *Emu*, *107*(4), 262. https://doi.org/10.1071/MU07026

Winger, B. M., Auteri, G. G., Pegan, T. M., & Weeks, B. C. (2019). A long winter for the Red Queen: rethinking the evolution of seasonal migration. *Biological Reviews*, *94*(3), 737–752. https://doi.org/10.1111/brv.12476

Winger, B. M., Barker, F. K., & Ree, R. H. (2014). Temperate origins of long-distance seasonal migration in New World songbirds. *Proceedings of the National Academy of*

Sciences, *111*(33), 12115–12120. https://doi.org/10.1073/pnas.1405000111

Winker, K., Withrow, J. J., Gibson, D. D., & Pruett, C. L. (2023). Beringia as a high-latitude engine of avian speciation. *Biological Reviews*, *98*, 1081–1099. https://doi.org/10.1111/brv.12945

Zhang, G., Li, C., Li, Q., Li, B., Larkin, D. M., Lee, C., Storz, J. F., Antunes, A., Greenwold, M. J., Meredith, R. W., Zeng, Y., Xiong, Z., Liu, S., Zhou, L., Huang, Z., An, N., Wang, J., Zheng, Q., Xiong, Y., … Wang, J. (2014). Comparative genomics reveals insights into avian genome evolution and adaptation. *Science*, *346*(6215), 1311–1321.

Zheng, X., Levine, D., Shen, J., Gogarten, S. M., Laurie, C., & Weir, B. S. (2012). A high-performance computing toolset for relatedness and principal component analysis of SNP data. *Bioinformatics*, *28*(24), 3326–3328. https://doi.org/10.1093/bioinformatics/bts606

Zink, R. M., & Gardner, A. S. (2017). Glaciation as a migratory switch. *Science Advances*, *3*(9), e1603133. https://doi.org/10.1126/sciadv.1603133

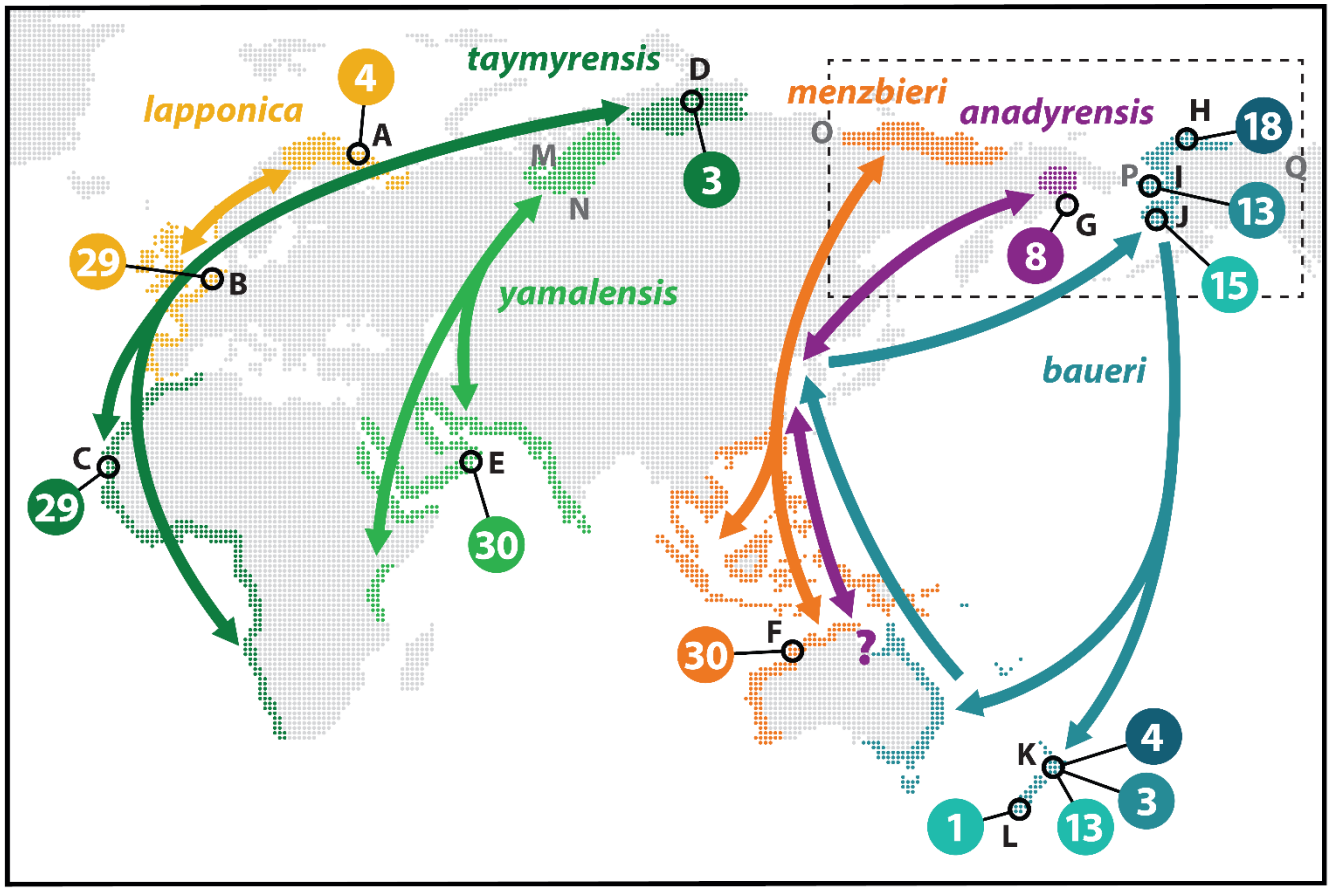

Figure 1. Global distribution and sampling of bar-tailed godwits. For each of six recognized subspecies (indicated by colour), arrows indicate general migration routes between northern breeding areas and southern non-breeding (i.e. boreal winter) areas (coloured areas). Numbers indicate total individuals sampled in each area (black circles); three shades of blue indicate sampling for *baueri* North, Central, and South. Letters refer to sampling sites (in black; see Table S1 for details) and other locations mentioned in the text (in gray): A, Murmansk, Russia; B, Wadden Sea, The Netherlands; C, Banc d'Arguin, Mauritania; D, Taimyr Peninsula, Russia; E, Barr al Hikman, Oman; F, Roebuck Bay, Australia; G, SE Chukotka, Russia; H, Colville River, Alaska; I, Seward Peninsula, Alaska; J, Yukon-Kuskokwim Delta, Alaska; K, North Island, New Zealand; L, South Island, New Zealand; M, West Siberian Lake; N, West Siberian Plain; O, Lena River Delta; P, Bering Land Bridge; Q, Mackenzie River Delta. Dashed box indicates approximate extent of the Beringia region.

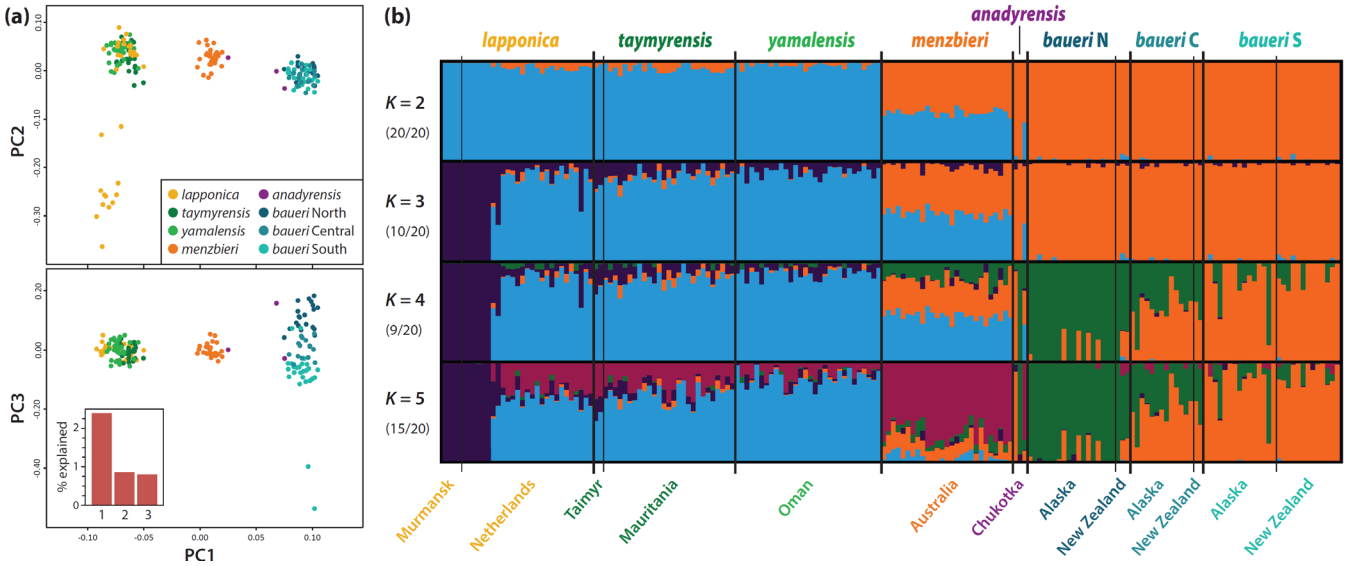

Figure 2. (a) Population structure estimated by principal component analysis. The individual scores (n = 184 individuals) for the first three principal components (PC1–3) are shown. The scree plot (inset) indicates the proportion of explained genetic variance by each PC, with PC1–3 explaining 4.0% of total variation. (b) Individual genetic ancestries assigned to major clusters for K = 2–5 estimated using ADMIXTURE. At each value of K, the ancestry proportions for the 184 individuals for the dominant solution were determined by CLUMPAK summary of 20 replicate runs. Numbers in parenthesis indicate proportion of replicate runs contributing to the dominant solution (see Figure S2 for minor clusters for K = 3–5). Names below plot indicate sampling locations (see Figure 1 and Table S1); colors indicate *a priori* purported breeding populations.

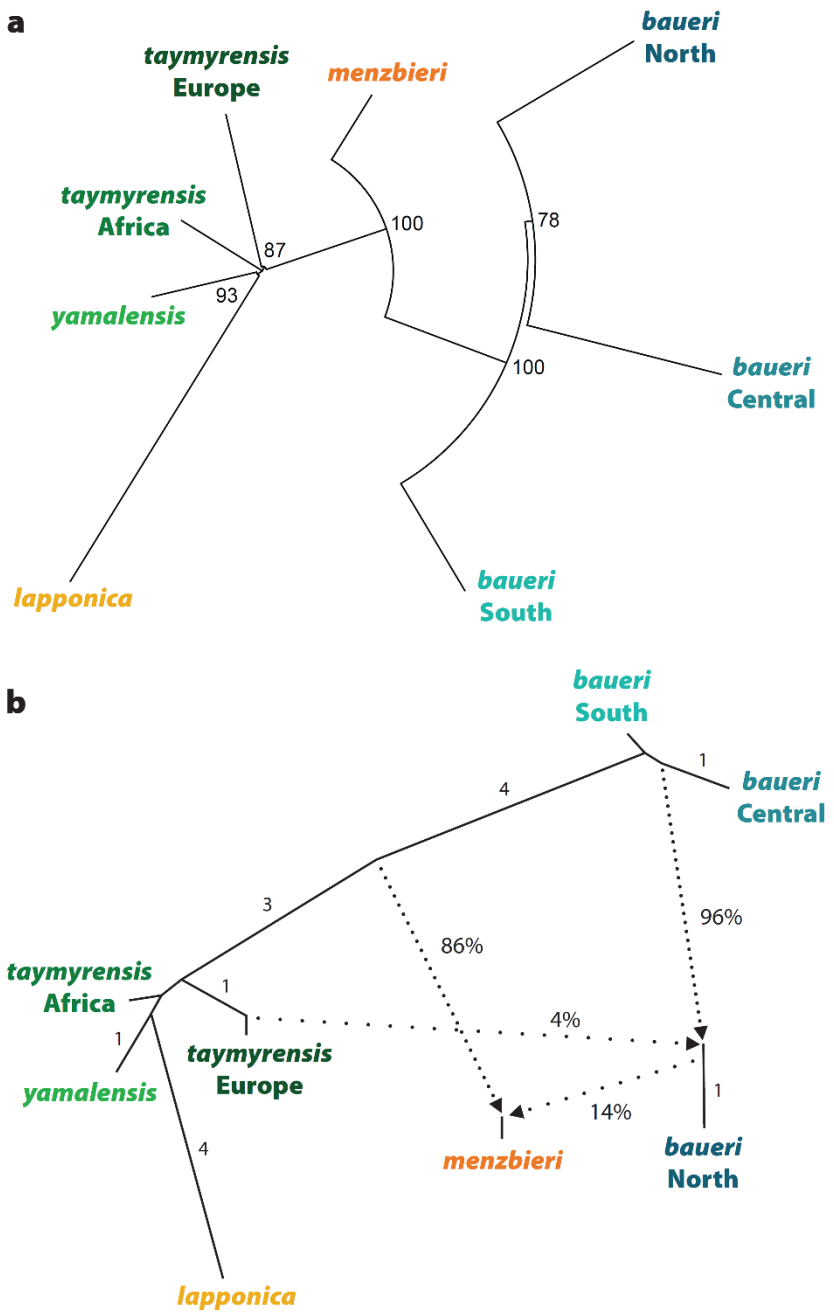

Figure 3. (a) Unrooted neighbour-joining tree, based on Nei's minimum distance. Numbers indicate bootstrapped node confidence (%). (b) AdmixtureGraph showing best graph with two migration reticulations ($m = 2$), arbitrarily rooted with *baueri* South population (see Methods). Numbers indicate relative genetic distances (unlabeled branches = 0 distance). Dotted lines represent admixtures, with percentages indicating admixture proportions, and arrows indicating direction of admixture.

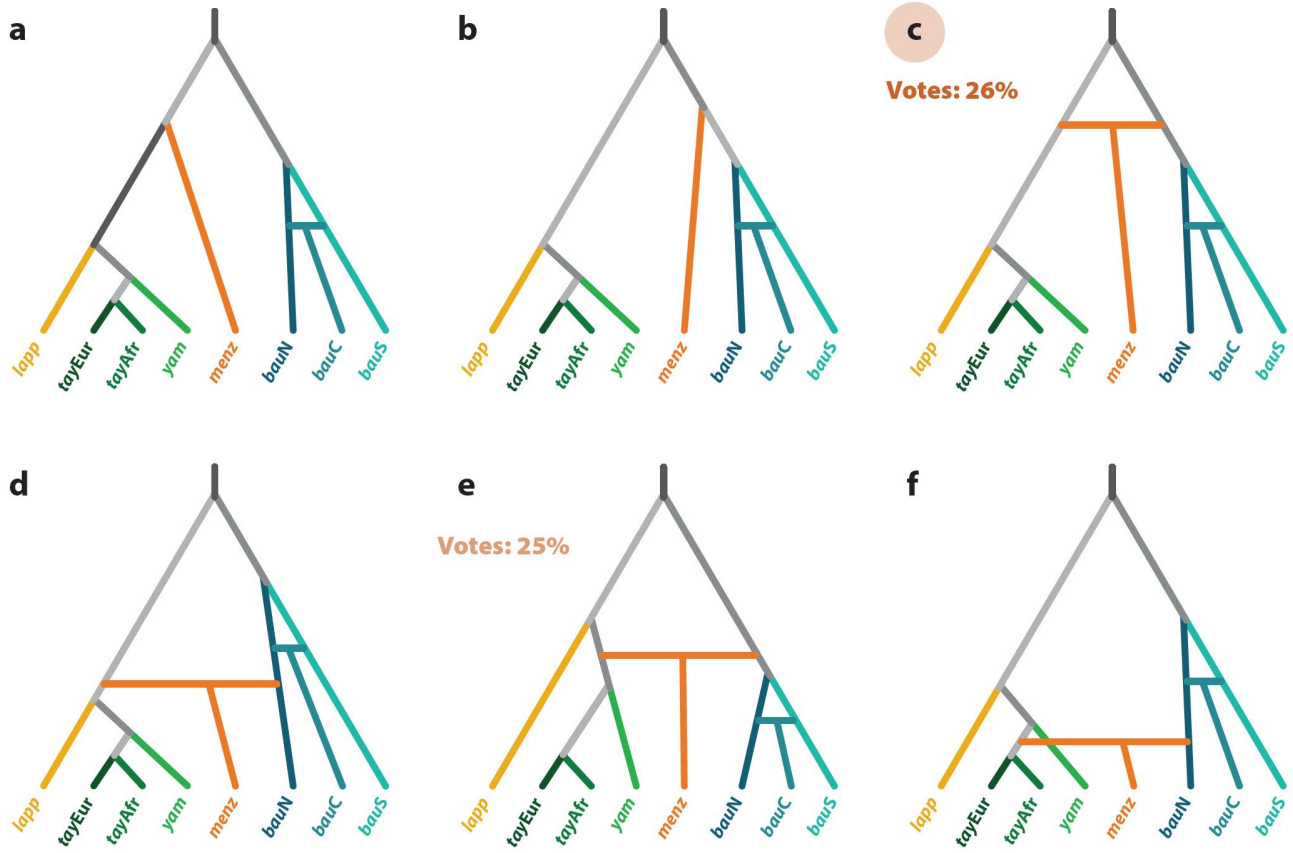

Figure 4. Scenarios tested in Step 2 of DIYABC-RF analysis: six possible scenarios for the origin of *menzbieri*, by either simple branching (a,b) or by admixture of the two main branches at relatively ancient (c), intermediate (d,e) or recent (f) time periods. Extant (sampled) populations are indicated by colours; inferred historical populations are shown in shades of grey. The best-supported scenario was (c), followed by (e), as inferred by the proportion of Random Forest classification votes; see Figure S5 and Tables S9 and S10 for details.

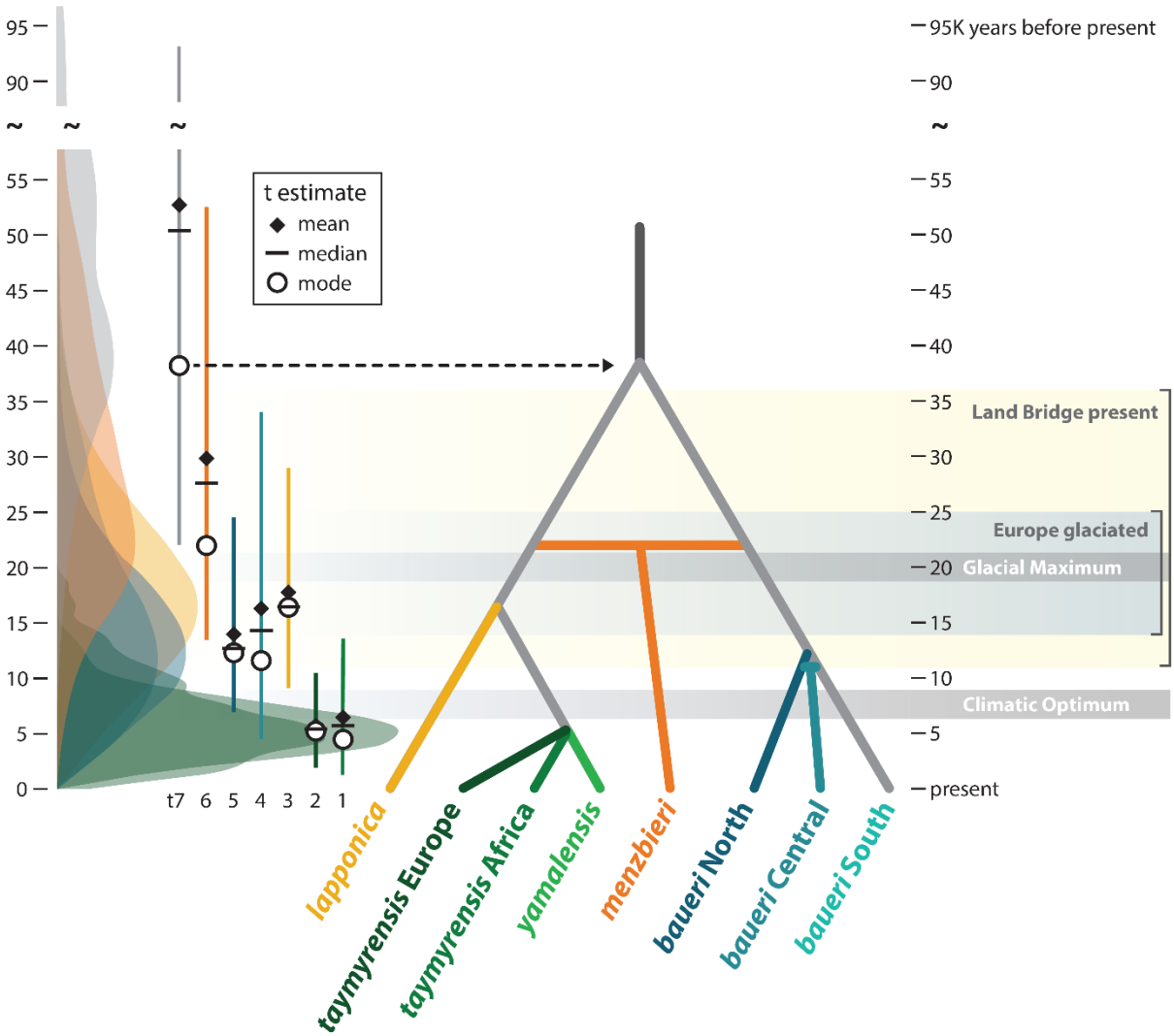

Figure 5. Best-supported Scenario in Step 2 of DIYABC-RF analysis (see Figure 4), scaled to relative time-parameter estimates (converted to years assuming a generation time of 8 years) for five divergence events (branches) and two admixture events (horizontal bars). On left, posterior distributions for each time parameter estimate, indicating mode, mean, median, and interval of 5th–95th quantiles (vertical line). For reference, estimated timing of Last Glacial Maximum, Holocene Climatic Optimum, and most recent presence of Bering Land Bridge and glaciation of Europe are shown.

Table 1. Mean population pairwise F_{ST} and 95% confidence intervals of estimates. All comparisons are significantly different from zero (1,000 permutations; $*p = 0.038$, $**p < 0.001$).

	lapponica	*taymyrensis* Europe	*taymyrensis* Africa	*yamalensis*	*menzbieri*	*baueri* North	*baueri* Central
***taymyrensis* Europe**	0.016**						
	[0–0.042]						
***taymyrensis* Africa**	0.014**	0.001*					
	[0–0.040]	[0–0.014]					
yamalensis	0.015**	0.003**	0.002**				
	[0.0003–0.040]	[0–0.016]	[0–0.010]				
menzbieri	0.026**	0.011**	0.010**	0.013**			
	[0.001–0.048]	[0.002–0.024]	[0.004–0.020]	[0.006–0.022]			
***baueri* North**	0.048**	0.032**	0.031**	0.034**	0.016**		
	[0.031–0.073]	[0.021–0.045]	[0.023–0.042]	[0.026–0.045]	[0.007–0.026]		
***baueri* Central**	0.047**	0.032**	0.031**	0.033**	0.015**	0.007**	
	[0.028–0.071]	[0.018–0.053]	[0.019–0.045]	[0.022–0.048]	[0.003–0.031]	[0–0.027]	
***baueri* South**	0.046**	0.031**	0.030**	0.033**	0.014**	0.009**	0.006**
	[0.030–0.070]	[0.021–0.044]	[0.024–0.040]	[0.026–0.040]	[0.007–0.024]	[0–0.020]	[0–0.023]